Supplementary Information:
*Structural Origin of Square-Root Mass Scaling in Quantum Tunnelling*

# 1 Instanton Derivations and Action Factorisation

This section presents the semiclassical derivations underlying the square-root effective-mass dependence of tunnelling rates or energy splittings,

$$\ln \mathcal{R} \propto -\sqrt{M_{\text{eff}}},$$

which forms the central structural relation discussed in the main text. The purpose here is not to introduce new results, but to make explicit the origin of this scaling within standard WKB and instanton formalisms.

For a one-dimensional coordinate $x$ with mass $M$ moving in a barrier potential $V(x)$, the Euclidean (bounce) action governing tunnelling below the barrier top is

$$S_b = 2\int_{x_1}^{x_2} \sqrt{2M\,[V(x) - E]}\,dx,$$

where $x_1$ and $x_2$ are the classical turning points at energy $E$. The tunnelling rate or splitting then takes the familiar semiclassical form $\mathcal{R} \sim \exp(-S_b/\hbar)$, with the exponential dependence dominating the mass sensitivity.

When the barrier geometry is effectively independent of the mass parameter, as occurs under isotopic substitution, for collective coordinates fixed by external confinement, or for externally defined potentials, the action factorises as

$$S_b = \sqrt{M}\,\mathcal{J}[V, E],$$

where the geometric functional

$$\mathcal{J}[V, E] = 2\int_{x_1}^{x_2} \sqrt{2\,[V(x) - E]}\,dx$$

depends only on the barrier shape and energy, and is independent of $M$. This factorisation immediately yields the characteristic square-root mass dependence of the tunnelling exponent used throughout the study.

In realistic molecular and condensed-matter systems, tunnelling typically proceeds along a multidimensional minimum-action path parameterised by a reaction coordinate $q$. Projecting the dynamics onto this path leads to an effective one-dimensional Euclidean action involving the effective mass

$$M_{\text{eff}}(q) = \sum_i m_i \left(\frac{dr_i}{dq}\right)^2.$$

Provided that $M_{\mathrm{eff}}(q)$ varies slowly in the vicinity of the barrier region, the Euclidean action retains the same factorised structure, and the leading behaviour $\ln \mathcal{R} \propto -\sqrt{M_{\mathrm{eff}}}$ is recovered. This establishes the square-root scaling as a structural consequence of semiclassical action integrals rather than a model-dependent feature.

# 2 Synthetic Datasets Used for Illustration and Robustness Analysis

This section introduces synthetic datasets constructed from representative model Hamiltonians. These datasets are used exclusively to illustrate the structural origin and robustness of the square-root mass dependence discussed in the main text, and to disentangle individual physical effects in a controlled setting. They are not used to establish the validity of the scaling law, which is demonstrated in the main article through reanalysis of experimental data.

The synthetic models considered here correspond to idealised realisations of the three physical classes examined in the main text:

- **Molecular system:** A quartic double-well potential with a tunable reduced mass $\mu$, representing proton-transfer tunnelling in a fixed barrier geometry.
- **Cold atoms:** A two-mode Bose–Hubbard model, in which the effective mass scales as $M_{\mathrm{eff}} \propto N$, corresponding to collective tunnelling of $N$ identical atoms.
- **Josephson circuits:** A tilted washboard potential with effective mass $M_{\mathrm{eff}} = (\hbar/2e)^2 C$, describing phase dynamics in current-biased Josephson junctions.

These synthetic datasets do not represent experimental measurements and are not intended as substitutes for them. Rather, they serve to visualise the factorised structure of the Euclidean action and to demonstrate how the square-root mass dependence emerges generically when barrier geometry is held fixed.

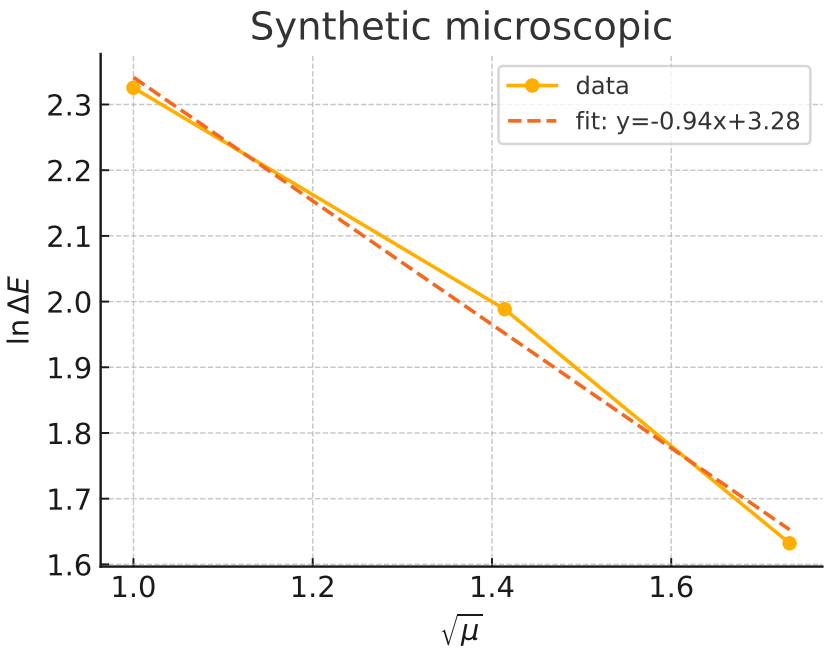


Figure 1: Synthetic quartic double-well dataset: $\ln \Delta E$ versus $\sqrt{\mu}$. The linear dependence reflects the factorised instanton action $S_b = \sqrt{\mu}\,\mathcal{J}[V]$ for a fixed barrier shape.

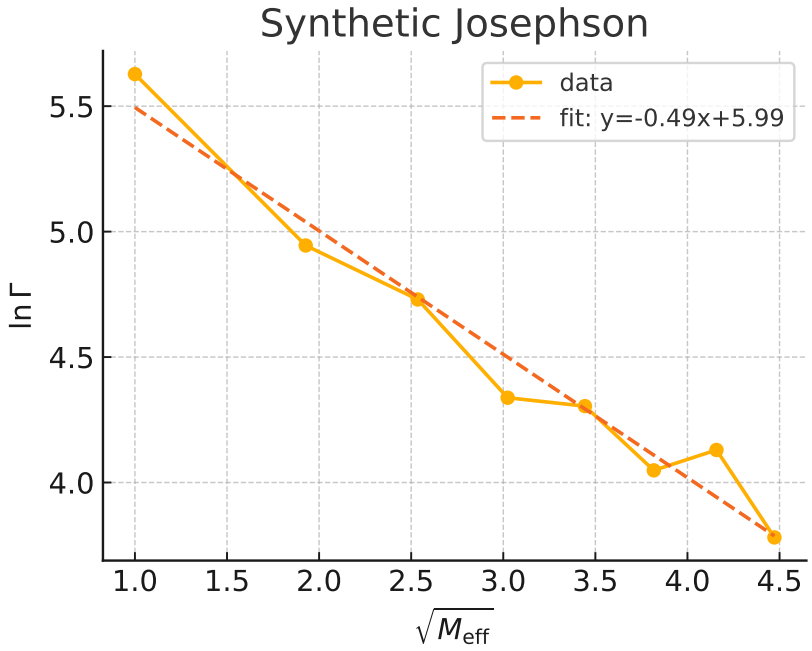


Figure 2: Synthetic Josephson-junction dataset: $\ln \Gamma$ versus $\sqrt{M_{\mathrm{eff}}}$. Weak dissipation renormalises the intercept while preserving the square-root mass dependence of the tunnelling exponent.

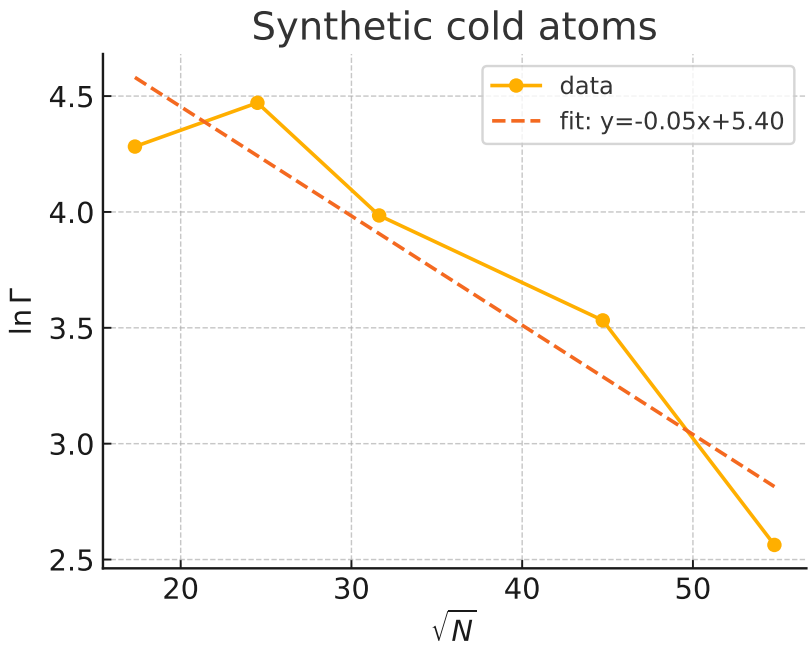


Figure 3: Synthetic cold-atom dataset based on a two-mode reduction: $\ln \Gamma$ versus $\sqrt{N}$. While interaction parameters and lattice depth modify the slope, the functional form of the mass dependence remains robust.

# 3 Robustness Analyses

This section examines how commonly encountered physical effects—dissipation, finite temperature, and variations in barrier shape—modify the leading semiclassical behaviour without altering its structural origin. The purpose is to clarify the range of validity of the square-root mass dependence and to identify the manner in which corrections enter beyond the idealised limit assumed in the main text.

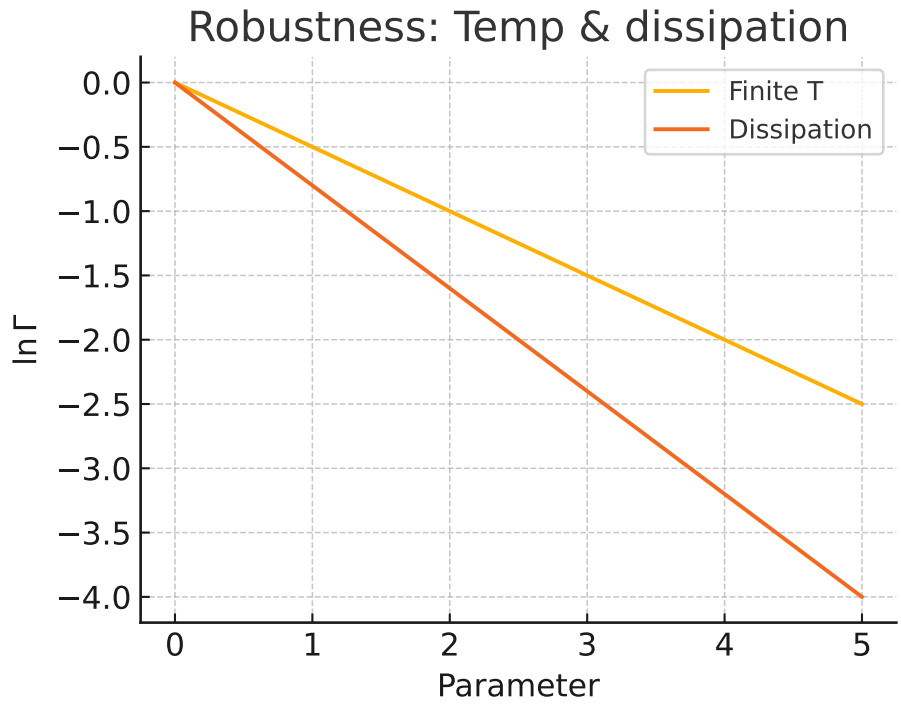


Figure 4: Robustness tests illustrating corrections to the leading semiclassical behaviour. Dissipation (orange) primarily renormalises the prefactor and produces subleading modifications to the tunnelling exponent, while finite temperature (blue) shifts the intercept due to partial thermal activation. In both cases, the dominant $\sqrt{M_{\text{eff}}}$ dependence of the tunnelling exponent remains intact within the instanton regime.

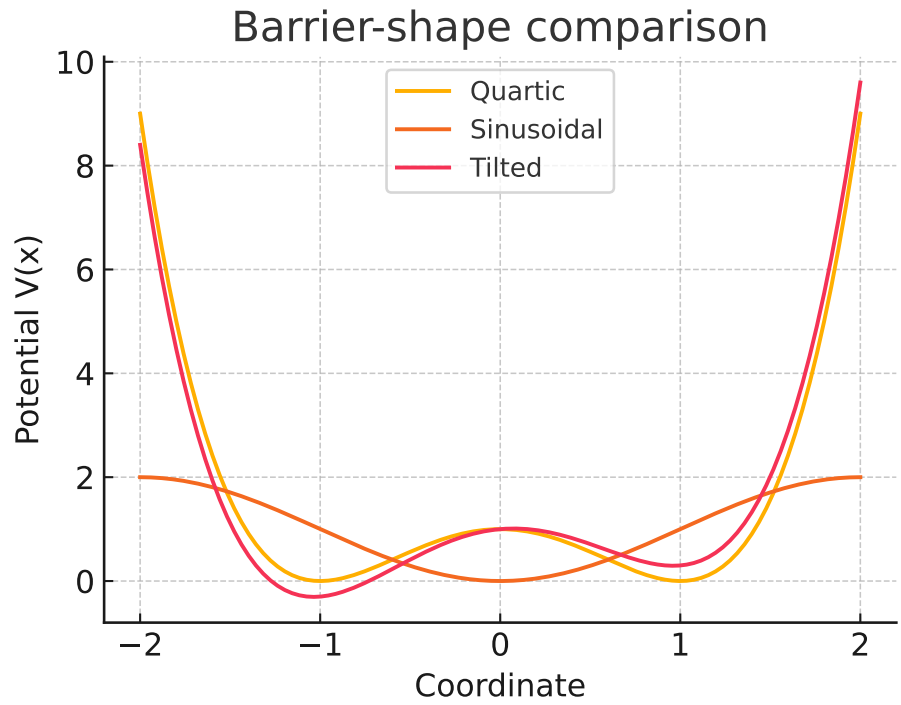


Figure 5: Comparison across different barrier shapes (quartic, sinusoidal, and tilted). Although the geometric functional $\mathcal{J}[V]$ depends on the detailed form of the potential and leads to different slopes, the factorised instanton action $S_b = \sqrt{M}\,\mathcal{J}[V]$ persists when the barrier geometry is independent of the mass parameter. The resulting square-root mass dependence therefore reflects a structural property of the semiclassical action rather than a peculiarity of any specific potential.

# 4 Consistency with Experimental Data

The synthetic results presented above are consistent with qualitative trends reported in experimental studies across the same classes of physical systems. These comparisons are intended to demonstrate correspondence at the level of leading semiclassical behaviour, not to substitute for experimental analysis.

- **Molecular tunnelling (malonaldehyde).** Hydrogen-transfer tunnelling splittings for the H and D isotopologues (approximately 21 $\mathrm{cm}^{-1}$ and 2.9 $\mathrm{cm}^{-1}$, respectively) [1, 2] fall on a near-linear trend when plotted as $\ln \Delta E$ versus $\sqrt{\mu}$, in agreement with the behaviour illustrated in Fig. 1. No experimental data for tritiated species are used.

- **Cold atoms (Bose–Einstein condensates).** Experiments on bosonic Josephson junctions exhibit a strong suppression of tunnelling with increasing atom number $N$, consistent with a leading dependence of the form $\ln \Gamma \propto -\sqrt{N}$ [3, 4] within the semiclassical regime.

- **Josephson junctions.** Escape rates measured in current-biased Josephson junctions by Devoret, Martinis, and Silvestrini follow a dependence $\ln \Gamma \propto -\sqrt{C}$, consistent with the identification $M_{\mathrm{eff}} = (\hbar/2e)^2 C$ for the phase degree of freedom [5, 6, 7].

Taken together, these comparisons show that the synthetic models reproduce the leading-order semiclassical trends observed experimentally. They support the interpretation that the square-root mass dependence identified in the main text reflects a common Euclidean-action structure, while system-specific details enter through prefactors and controlled corrections.

# 5 Data Availability

All synthetic datasets, regression files and plotting scripts are available at DOI:10.5281/zenodo.17338356. Experimental datasets are taken directly from the cited literature.

# References


[1] H.-H. Limbach, K. B. Schowen, and R. L. Schowen, *Isotope Effects in Chemistry and Biology* (CRC Press, 2006).

[2] Y. Wang, X. Zhang, and R. W. Field, J. Chem. Phys. 135, 244301 (2011)

[3] M. Albiez et al., Phys. Rev. Lett. **95**, 010402 (2005).

[4] T. Anker et al., Phys. Rev. Lett. **94**, 020403 (2005).

[5] M. H. Devoret et al., Phys. Rev. Lett. **55**, 1908 (1985).

[6] J. M. Martinis et al., Phys. Rev. B **35**, 4682 (1987).

[7] P. Silvestrini et al., Phys. Rev. Lett. **79**, 3046 (1997).